Available online at www.sciencedirect.com
SCIENCE DIRECT®
Journal of Power Sources 137 (2004) 53–61
JOURNAL OF POWER SOURCES
www.elsevier.com/locate/jpowsour

Development of a microreactor for the production of hydrogen from ammonia

J.C. Ganley, E.G. Seebauer, R.I. Masel*

Department of Chemical and Biomolecular Engineering, University of Illinois at Urbana-Champaign, 213 Roger Adams Laboratory, Box C-3, 600 S. Mathews Avenue, Urbana, IL 61801-3792, USA

Received 24 April 2004; accepted 20 May 2004
Available online 27 July 2004

Abstract

This paper describes the development of a structured aluminum-anodized alumina microreactor that exhibits high catalytic activity for the decomposition of anhydrous ammonia to nitrogen and hydrogen at moderate temperatures. Modifications such as adjustments to the geometry of the microreactor features, surface area enhancement of the anodized catalyst support, choice of Ru precursor, and application of a catalyst promoter are each shown to affect the reactor performance to varying degrees. The reactor converts 99% of ammonia at 600 °C into the equivalent of 60 W of hydrogen. These numbers are sufficient for to merit serious consideration for use in practical applications, particularly in mobile devices fueled by hydrogen where monolithic structures are advantageous.
© 2004 Elsevier B.V. All rights reserved.

Keywords: Microreactor; Hydrogen production; Ammonia reforming

1. Introduction

In recent years, there has been a sharp increase in the study of chemical reactors far smaller than those commonly used in industry today [1–3]. The promise of meso- and microreactors rests upon the many possible advantages that small scale reactors possess compared to their larger, conventional counterparts. These advantages include improved heat and mass transfer due to smaller characteristic lengths, improved reaction efficiency due to higher surface-to-volume ratios, and ease of use in portable applications due to reduced volume. Recent interest in powering fuel cells for small, portable electronic devices [4–6] has provided particular impetus for research on microreactors for the production of hydrogen. The catalytic decomposition of ammonia is widely viewed as an attractive source of hydrogen for fuel cells [7–10]. Ammonia is readily available, has a high energy content, exhibits a narrow explosion limit, and decomposes relatively easily with no need for added steam or oxygen. These advantages make ammonia particularly suited for portable power applications. The best catalysts for this reaction are generally metals such as Ru or Ni supported on oxides such as alumina. Unfortunately, conventional catalyst particles loaded into a microreactor suffer from problems with excessive pressure drop, mechanical attrition, and poor heat transfer. To circumvent these problems, we have developed a microreactor configuration based on an aluminum body. The aluminum oxide catalyst support is formed by anodization of the reactor interior. Suitable machining of the reactor interior prior to anodization reduces pressure drop, and the intimate contact between the oxide layer and reactor body mitigates problems with mechanical attrition and heat transfer. Previously, we have demonstrated the operation of such a microreactor for ammonia decomposition to produce hydrogen [7,11].

One disadvantage of this design, however, stems from the low melting point (661 °C) of the aluminum body. Operation is definitely limited to below 650 °C, and reliability considerations suggest operation significantly lower than that – probably no more than 600 °C. For many portable applications, the microreactor must be capable of producing the hydrogen equivalent of roughly 20 W of electrical power, and the reactor volume must remain below about 0.5 cm^3 in order to avoid unacceptably large overall device sizes. To use the ammonia reactant efficiently and to avoid having to capture large amounts of unreacted ammonia out of the exhaust, such reactors must be capable of high conversions of ammonia >99%. The previous reactor reported by this group had a volume near 0.3 cm^3, but produced hydrogen equivalent to only 13 W of power with a conversion of just 85% at 650 °C. Although these numbers were encouraging, they clearly did not meet the requirements for a practical microreactor.

* Corresponding author. Tel.: +1 217 333 6841; fax: +1 217 333 5052.
E-mail address: r-masel@uiuc.edu (R.I. Masel).

0378-7753/$ – see front matter © 2004 Elsevier B.V. All rights reserved.
doi:10.1016/j.jpowsour.2004.05.032

The present study examines the effects of several potential improvements to the reactor configuration and fabrication, including changing the geometry to a channel structure, reducing key reactor dimensions, and employing different catalyst preparation procedures. The results show that each change produces only modest improvements in reactor conversion. However, in aggregate, the changes permit the production of hydrogen equivalent to 60 W with an ammonia conversion of 99% at 600 °C—all in a volume of 0.35 cm^3. This result satisfies the performance requirements of practical reactors much more closely.

2. Experimental

2.1. Reactor fabrication

Aluminum microreactors were constructed from rolled bar stock of 1100 aluminum (>99% Al). Electrical discharge machining (EDM) was employed to cut 3 mm deep grooves into the substrate to form either an array of square posts (Fig. 1) or a series of parallel channels (Fig. 2). The post reactor was 9.2 mm wide, 9.2 mm long, and 4 mm thick. Each post was 300 μm wide, and the distance between posts was 260 μm. Channel reactors were 9.2 mm wide, 12.6 mm long, and 4 mm thick. Fourteen parallel channels stretched along the reactor length. Two types of channel reactors were constructed. The "standard" design incorporated channels that were 260 μm wide, separated by walls 175 μm thick. In the "reduced-width" design, each channel was 140 μm wide, with walls 300 μm thick.

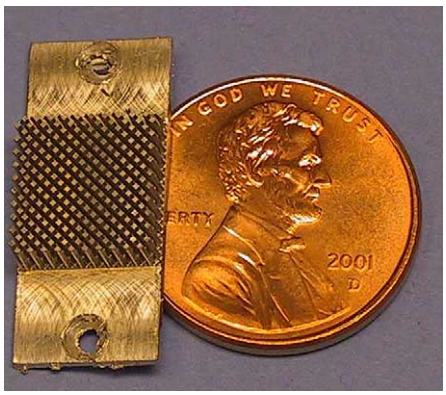

Fig. 1. Photograph of a post reactor beside a US penny.

Fig. 2. Photograph of a standard channel reactor beside a US penny.

The reactors were degreased in acetone, and then anodized at 30 V for 30 min in a 0.6 M oxalic acid solution maintained at 18 °C. The thin anodic film was then removed by immersion in a 1.5 wt.% chromic acid and 6 wt.% phosphoric acid solution at 60 °C for 15 min. Removal of this first anodic film allowed a second, thicker film to be grown on a surface free of the defects and scratches characteristic of the starting material. The reactors were re-anodized for 16 h and dried in a convection oven at 150 °C for 4 h. One of the standard channel reactors was also treated one or more times in the following manner: immersion in deionized water at 100 °C for 1 h, drying in a convection oven at 150 °C for 30 min, and then dehydration at 550 °C in a tube furnace under air for 16 h.

The total surface area of each reactor was determined using single-point BET with a commercial unit (Micromeritics ChemiSorb 2705), with nitrogen physisorption at 77 K. The total pore volume was estimated by the weighing the reactor before and after immersion in deionized water at room temperature.

2.2. Reactor catalyzation and testing

Ruthenium catalyst was deposited onto the anodized reactors by wet impregnation with either 0.66 M $RuCl_3$ in 75% acetone/25% water or 0.11 M ruthenium(III) acetylacetonate in 2,4-pentanedione. The reactors were dried in a convection oven at 150 °C for 1 h and calcined in a tube furnace under air for 4 h at 550 °C. In order to achieve a similar weight of ruthenium catalyst (∼3.5 wt.%) from both solutions, the reactor using ruthenium(III) acetylacetonate was impregnated, dried, and calcined six times. Following calcination, one reactor impregnated with $RuCl_3$ was dipped into an aqueous 0.39 M solution of KNO_3 to achieve a potassium loading of ∼0.8 wt.% on the alumina. Prior to testing, the reactors were reduced in hydrogen at 550 °C for 2 h. Active metal dispersion for each reactor was calculated using pulsed CO adsorption at room temperature in a commercial unit (Micromeritics ChemiSorb 2705).

Catalyst reactivity was measured in a quartz tube heated by a temperature-controlled tube furnace. A few alumina pellets placed upstream of the reactor housing served as a reactant preheater. Concentrations in the product stream were monitored by passing all reactor effluent through an on-line thermal conductivity detector. The detector was calibrated by passing known mixtures of ammonia, hydrogen, and nitrogen through the reactor bypass. Control experiments throughout the temperature range of interest showed that the reactor housing induced no conversion in the absence of catalyst.

The reactant stream of technical grade (99.99%) anhydrous ammonia was controlled with a calibrated mass flow meter. All experiments were carried out at atmospheric pressure.

Table 1
Microreactor characteristics

	Reactor designation						
	A	B	C	D	E	F	G
Reactor type	Channel	Post	Channel	Channel	Channel	Channel	Channel
Post gap or channel width (μm)	260	260	140	260	260	260	140
Hydrothermal–thermal treatment	N	N	N	Y	N	N	Y
Catalyst precursor	$RuCl_3$	$RuCl_3$	$RuCl_3$	$RuCl_3$	Ru(acac)	$RuCl_3$	$RuCl_3$
Potassium promoter	N	N	N	N	N	Y	Y
Reactor surface area (m^2)	2.50	1.72	2.40	26.11	2.54	2.44	26.07
Ru catalyst dispersion (%)	15	16	14	25	4	15	28
Temperature for 95% conversion of 145 sccm NH_3 feed (°C)	625[a]	658[b]	595[a]	602[a]	735[c]	593[a]	554[a]
Conversion of 145 sccm NH_3 feed at 525 °C	0.68	0.51	0.75	0.72	0.15	0.78	0.88

[a] Interpolated using experimental data.
[b] Extrapolated using experimental data.
[c] Extrapolated using experimental data, value is greater than the melting point of aluminum.

3. Results and discussion

Table 1 summarizes the characteristics of each of the seven reactors studied. Reactor A represented the base case: a standard channel reactor impregnated with $RuCl_3$, no potassium promoter, and no hydrothermal–thermal treatment of the oxide.

3.1. Feature geometry: post vs. channel reactors

Earlier work [7,11,12] with the post configuration of Fig. 1 uncovered two significant problems. First, the anodic oxide tended to delaminate from sharp features such as the edges of square posts [7,11]. Thicker oxides, which offer greater total surface areas, worsened the delamination. Second, a computational study of this reactor type [12] showed significant undesirable backmixing under slow ammonia flow conditions that reduced reactant conversion because of the first-order kinetics. By eliminating square posts, the standard channel configuration seeks to reduce the number of sharp features as well as the degree of backmixing.

Reactors A (channels) and B (posts) in Table 1 were designed to have similar ratios of surface area to interior volume, as well a similar dispersions of the Ru catalyst (15%). Reactor A had a support surface area of 2.50 m^2 in a volume of 0.35 cm^3, leading to a surface-to-volume ratio of 7.1 m^2/cm^3. Reactor B had a support surface area of 1.72 m^2 in a volume of 0.25 cm^3, for a nearly identical surface-to-volume ratio of 6.9 m^2/cm^3. The thick oxides formed on these structures exhibited limited film cracking at sharp features in a similar fashion to those studied previously [7,11], but this cracking occurred only at the ends of the channel reactor, compared to each of the corners of every square post in the post reactor.

Fig. 3 shows the fractional conversion of a 145 sccm anhydrous ammonia feed to reactors A and B at various reactor temperatures. The reactors exhibited similar ammonia conversions at low and high temperatures (where conversions are near zero and unity, respectively). However, at 525 °C, the channel reactor yielded significantly greater conversions: roughly 0.68 versus 0.51 for the post reactor. Thus, a basic premise of the channel design was confirmed: that reduced backmixing would increase conversion.

3.2. Feature geometry: reduction in channel width

The heat and mass transfer benefits gained by reducing the characteristic dimensions of heterogeneous microreactors are well known [13,14]. In particular, smaller diffusion distances in the gas phase promote decreased diffusion resistances for reactions that are not completely controlled by surface kinetics on the catalyst. Such kinetics have not been completely worked out for ammonia decomposition on Ru, however. To test whether diffusion resistances play a role, reactor C was constructed in a channel configuration, with the channel width nearly half that of the standard channel reactor.

Reactors A and C in Table 1 were designed to have similar ratios of surface area to interior volume, as well a similar dispersions of the Ru catalyst (15%). Reactor A had a support surface area of 2.50 m^2 in a volume of 0.35 cm^3, leading to a surface-to-volume ratio of 7.1 m^2/cm^3. Reactor C had a support surface area of 2.40 m^2 in a volume of 0.35 cm^3, for a nearly identical surface-to-volume ratio of 6.9 m^2/cm^3.

Fig. 4 shows the fractional conversion of a 145 sccm anhydrous ammonia feed to reactors A and C at various reactor temperatures. The reactors exhibited similar ammonia conversions at low and high temperatures (where conversions are near zero and unity), respectively. However, at 525 °C, the reactor with smaller channels yielded slightly greater conversions: roughly 0.75 versus 0.68 for the standard reactor. Thus, it appears that diffusion resistances do indeed play a role in this reaction, and can be mitigated by smaller reactor dimensions.

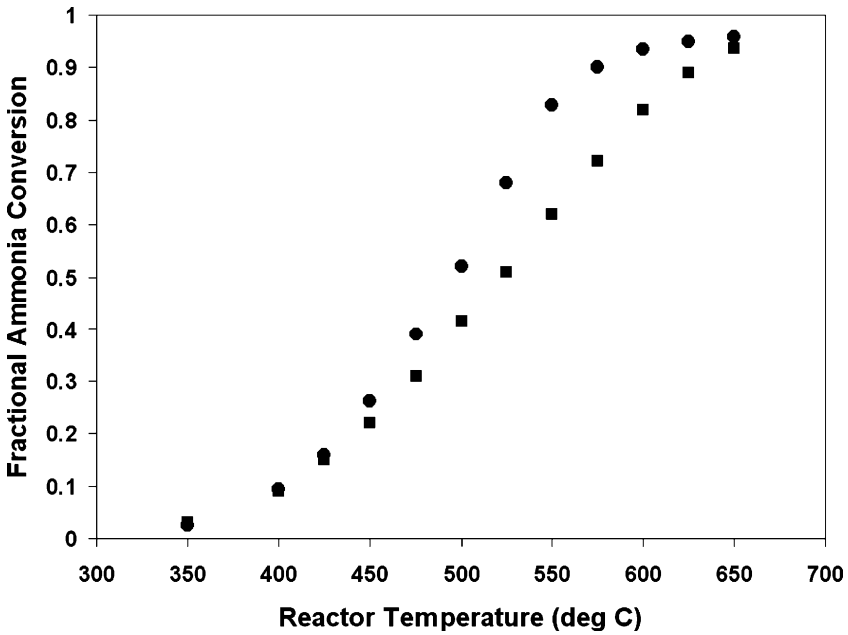

Fig. 3. Fractional conversion of 145 sccm anhydrous ammonia over Ru-catalyzed microreactors of (●) 260 μm channel width and (■) 260 μm post-gap configurations at various temperatures.

3.3. Catalyst support: hydrothermal–thermal treatment of oxide film

Alumina may be treated with steam or boiling water to produce a hydrated alumina hydroxide [15–18]. Importantly for the present work, these hydrated alumina hydroxides may be converted upon dehydration to the high-surface area δ- or γ-alumina phases under the proper conditions [19], allowing significant increases in the specific and total oxide surface areas [20]. To test whether such a treatment of the porous alumina films used in this study could enhance reactor performance, reactor D was subjected to a single hydrothermal–thermal treatment as described in the experimental section.Reactors A and D in Table 1 were prepared as standard channel reactors with identical volumes and channel dimensions. Reactor A had a support surface area of 2.50 m^2 in a volume of 0.35 cm^3, leading to a surface-to-volume ratio of 7.1 m^2/cm^3. Reactor D had a

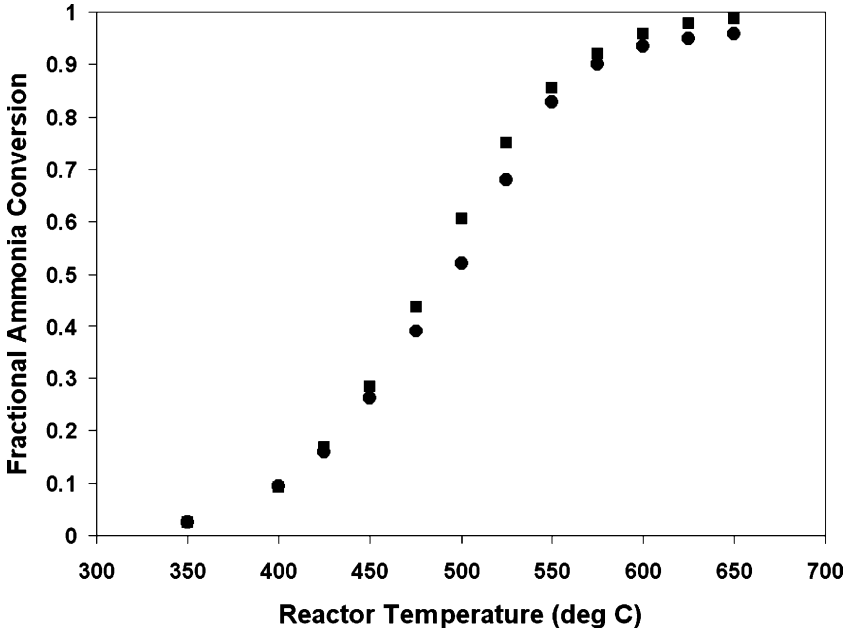

Fig. 4. Fractional conversion of 145 sccm anhydrous ammonia over Ru-catalyzed microreactors of (●) 260 μm channel width and (■) 140 μm channel width at various temperatures.

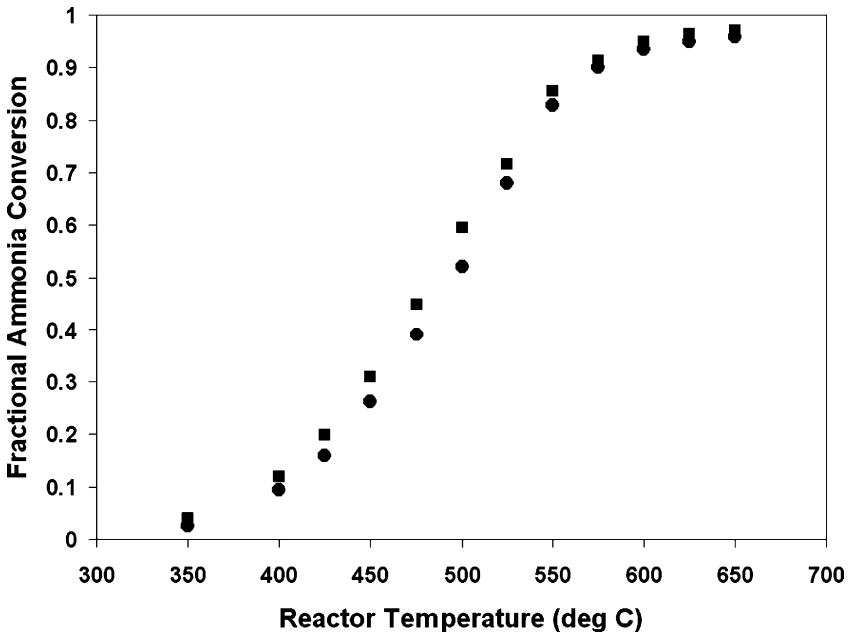

Fig. 5. Fractional conversion of 145 sccm anhydrous ammonia over 260 μm channel width, Ru-catalyzed microreactors with (●) no hydrothermal–thermal surface treatment and (■) a single hydrothermal–thermal surface treatment.

support surface area of 26.11 m^2 in a volume of 0.35 cm^3, for a much higher surface-to-volume ratio of 75 m^2/cm^3. Reactor D also had an increased dispersion of the Ru catalyst (25% vs. 15% for reactor A).

Fig. 5 shows the fractional conversion of a 145 sccm anhydrous ammonia feed to reactors A and D at various reactor temperatures. At 525 °C, the reactor with hydrothermal–thermally treated support yielded slightly greater conversions: roughly 0.72 versus 0.68 for the standard reactor. Thus, it appears that the larger support surface area and increased catalyst dispersion due to hydrothermal–thermal treatment may enhance reactor performance.

3.4. Catalyst precursor: organometallic vs. metal halide

Homogeneous and supported ruthenium catalysts are often prepared from both organometallic precursors [21–23] and aqueous or organic solvent solutions of $RuCl_3$ [24,25]. Generally, solutions of much higher Ru concentration can be made using a $RuCl_3$ precursor, but the resulting residual surface chlorides can be poisons for some heterogeneous catalytic reactions [23]. To test the effect of the precursor used in the catalyzation of the microreactor, reactor E was constructed as a standard channel reactor catalyzed with ruthenium(III) acetylacetonate for comparison with reactor A; which was catalyzed with $RuCl_3$.

Reactors A and E in Table 1 were prepared as standard channel reactors with identical volumes, surface oxide, and channel dimensions. Reactor A had a support surface area of 2.50 m^2 in a volume of 0.35 cm^3, leading to a surface-to-volume ratio of 7.1 m^2/cm^3. Reactor E had a support surface area of 2.54 m^2 in a volume of 0.35 cm^3, for a nearly identical surface-to-volume ratio of 7.3 m^2/cm^3. Reactor E had a much lower dispersion of the Ru catalyst (4% versus 15% for reactor A).

Fig. 6 shows the fractional conversion of a 145 sccm anhydrous ammonia feed to reactors A and E at various reactor temperatures. The conversion of the reactor impregnated with $RuCl_3$ precursor was far higher than that of the reactor made using ruthenium(III) acetylacetonate at all temperatures considered. At 525 °C, the $RuCl_3$-catalyzed reactor yielded a much higher conversion: roughly 0.68 versus 0.15 for the reactor made using ruthenium(III) acetylacetonate. The higher metal dispersion achieved with a $RuCl_3$ precursor produced a reactor that was far superior to one catalyzed with the organometallic precursor ruthenium(III) acetylacetonate, even with an equivalent catalyst loading (~3.5 wt.%).

3.5. Catalyst modification: potassium promoter

Alkali and alkaline earth catalyst promoters are important in the production of Fe-and Ru-based ammonia synthesis catalysts [26–30]. In particular, potassium in the form of potash (K_2O) has shown a strong promotion effect in these catalysts by increasing the reaction rate in the appropriate pressure and temperature regimes for both ammonia formation and decomposition. For Ru catalysts, addition of potassium causes no significant increase in dispersion regardless of the support used [30–33]. The catalytic rate improvement is attributed largely to electronic promotion. To test the utility of potassium promotion, reactor F was constructed as a standard channel reactor catalyzed with 3.5 wt.% Ru and promoted with 0.8 wt.% K from KNO_3.

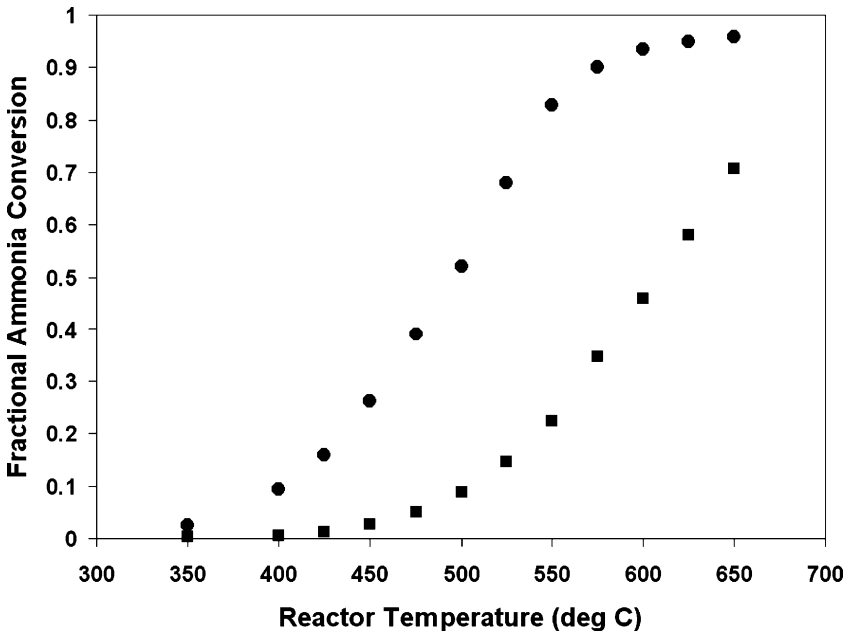

Fig. 6. Fractional conversion of 145 sccm anhydrous ammonia over 260 μm channel width, Ru-catalyzed microreactors made using (●) $RuCl_3$ precursor and (■) ruthenium(III) acetylacetonate precursor, for a total Ru loading of ~3.5 wt.% in each case.

Reactors A and F in Table 1 were prepared with identical volumes, surface oxide, and channel dimensions. Reactor A had a support surface area of 2.50 m^2 in a volume of 0.35 cm^3, leading to a surface-to-volume ratio of 7.1 m^2/cm^3. Reactor F had a support surface area of 2.44 m^2 in a volume of 0.35 cm^3, for a nearly identical surface-to-volume ratio of 7.0 m^2/cm^3. Reactor F had the same dispersion of Ru (15%) as reactor A.

Fig. 7 shows the fractional conversion of a 145 sccm anhydrous ammonia feed to reactors A and F at various reactor temperatures. The reactor with potassium promoter yielded greater conversions at 525 °C: roughly 0.78 versus 0.68 for the non-promoted reactor. This increased activity suggests that the addition of a potassium promoter has a positive effect on reactor behavior, despite the lack of change in catalyst dispersion.

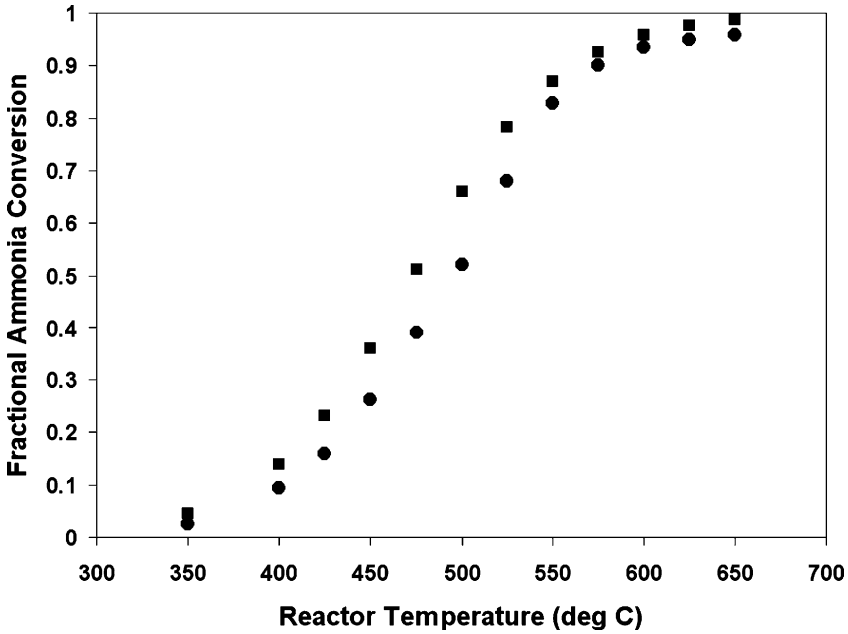

Fig. 7. Fractional conversion of 145 sccm anhydrous ammonia over 260 μm channel width, Ru-catalyzed microreactors made with (■) potassium promoted Ru catalyst or (●) unpromoted Ru.

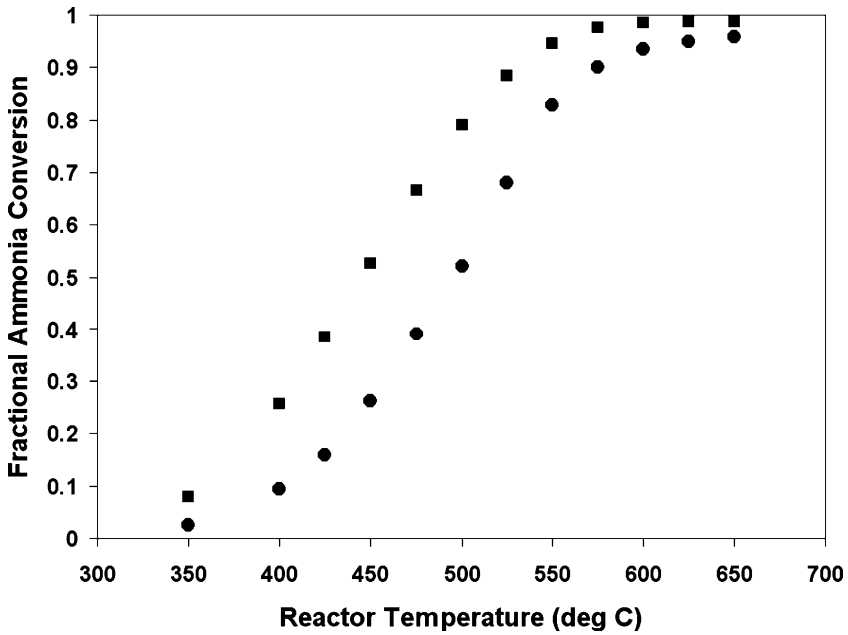

Fig. 8. Fractional conversion of 145 sccm anhydrous ammonia over channel reactors prepared using $RuCl_3$ with (●) 260 μm channel width, no hydrothermal–thermal treatment, unpromoted Ru catalyst and (■) 140 μm channel width, hydrothermal–thermally treated, promoted Ru catalyst.

3.6. Aggregate improvements

The previous sections have examined the impact of various reactor modifications individually; including reactor geometry, catalyst support treatment, catalyzation precursor selection, and catalyst promotion. Here, we compare the characteristics and performance of a microreactor enhanced with all of these modifications applied simultaneously (reactor G), with the standard channel reactor (reactor A).

Reactor G was a potassium promoted, support treated, reduced channel-width microreactor with a support surface area of 26.07 m^2 in a reactor volume of 0.35 cm^3, or a surface-to-volume ratio of 74 m^2/cm^3. Reactor A, which was had no potassium promoter, no support treatment, and a standard channel width occupied a reactor volume of 0.35 cm^3 with a support surface area of 2.50 m^2 for a much lower surface area to volume quotient of 7.1 m^2/cm^3. Reactor G had a higher dispersion of the Ru catalyst (28% versus 15% for reactor A).

Fig. 8 shows the fractional conversion of a 145 sccm anhydrous ammonia feed to reactors A and G at various reactor temperatures. At 525 °C, the summarily improved reactor yielded a higher conversion: 0.88 versus 0.68 for the standard channel reactor. Not surprisingly, reactor G outperformed all other reactor configurations tested in the present study. At 600 °C and a 145 sccm ammonia feed, reactor G achieved a conversion of about 0.99 and produces over 200 sccm, or about 60 W, of hydrogen.

Reactor G converted 99% of a 145 sccm ammonia feed at a reactor temperature of 650 °C. This represents an enormous improvement compared to the results of our first generation microreactor study [7,11], in which an anodized post reactor with ruthenium(III) acetylacetonate-derived catalyst converted only 42% of the ammonia feed at the same feed rate and temperature.

4. Conclusions

The results presented here demonstrated significant improvements in a structured aluminum-anodized alumina microreactor for ammonia decomposition. Modifications such as adjustments to the geometry of the microreactor features, surface area enhancement of the anodized catalyst support, choice of Ru precursor, and application of a catalyst promoter were each shown to affect the reactor performance to varying degrees. In aggregate, the changes permit the production of hydrogen equivalent to 60 W with an ammonia conversion of 99% at 600 °C—all in a volume of 0.35 cm^3. This performance exceeds the specifications for practical use laid out in the Introduction. Of course, a reactor operating in the real world forms part of a system that requires a compact heating source and must meet other performance and reliability criteria not discussed in this paper. However, it is now safe to say that microreactors for practical hydrogen production in significant applications have progressed to the point where the reactors considered in isolation can satisfy several of the most fundamental criteria needed for useful operation.

Furthermore, the methods described in this study do not exhaust all the possibilities for further improvements. Moving to a construction material with a higher melting temperature than aluminum would permit operation at higher

temperatures and yield faster rates. However, the relative simplicity of creating a robust catalyst support by anodization would be lost. Improvements may be possible even with aluminum construction, however. For example, many commercial catalysts are doubly or even triply promoted. While the potassium ion obviously enhances the rate, further promotion may be possible with the addition of other electronic promoters such as Ca, Cs, or Mg; all of which are common in ammonia synthesis catalysts. To our knowledge, Ru is the most effective catalyst for ammonia decomposition. It is conceivable, however, that bimetallic combinations of various transition metal catalysts may exceed the activity of Ru, as has been observed with CoMo nitride bimetallic catalysts in ammonia synthesis with respect to Fe and Ru [34,35].

Acknowledgements

This work was supported by the Department of Defense Multidisciplinary University Research Initiative (MURI) program administered by the Army Research Office under contract DAAD19-01-1-0582. Any opinions, findings, and conclusions or recommendations expressed in this publication are those of the authors and do not necessarily reflect the views of the Department of Defense or the Army Research Office.

References

[1] T. McCreedy, N. Wilson, Microfabricated reactors for on-chip heterogeneous catalysis, Analyst 126 (2001) 21.
[2] P. Claus, D. Hnike, T. Zech, Miniaturization of screening devices for the combinatorial development of heterogeneous catalysts, Catal. Today 67 (2001) 319.
[3] S. Ajmera, C. Delattre, M. Schmidt, K. Jensen, Microfabricated cross-flow chemical reactor for catalyst testing, Sens. Actuators B 82 (2002) 297.
[4] C. Call, Proceedings palm power workshop, Panama City FL, Motorola move communications towards the miniature fuel cell, Electron. Eng. 72 (2000) 9.
[5] R. Neale, Motorola move communications towards the miniature fuel cell, Electron. Eng. 72 (2000) 72.
[6] R. Srinivasan, I.M. Hsing, P.E. Berger, K.F. Jensen, S.L. Firebaugh, M.A. Schmidt, M.P. Harrold, J.J. Lerou, J.F. Ryley, Micromachined reactors for catalytic partial oxidation reactions, AIChE J. 43 (1997) 3059.
[7] J. Ganley, E. Seebauer, R. Masel, Porous anodic alumina microreactors for production of hydrogen from ammonia, AIChE J. 50 (2004) 829.
[8] R. Metkemeijer, P. Achard, Ammonia as a feedstock for a hydrogen fuel cell reformer and fuel cell behavior, J. Power Sources 49 (1994) 271.
[9] T. Choudhary, C. Sivadinarayana, D. Goodman, Catalytic ammonia decomposition: CO_x-free hydrogen production for fuel cell applications, Catal. Lett. 72 (2001) 197.
[10] A. Chellappa, C. Fischer, W. Thomson, Ammonia decomposition kinetics over Ni–Pt/Al_2O_3 for PEM fuel cell applications, Appl. Catal. A: Gen. 227 (2002) 231.
[11] J.C. Ganley, E.G. Seebauer, R.I. Masel, Microreactors for fuel conversion, in: Proceedings of the 40th Power Sources Conference, vol. 367, 2002.
[12] S. Deshmukh, A. Mhadeshwar, D. Vlachos, Microreactor modeling for hydrogen production from ammonia decomposition on ruthenium, Ind. Eng. Chem. Res. ACS ASAP (2004).
[13] D. Beard, Taylor dispersion of a solute in a microfluidic channel, J. Appl. Phys. 89 (2001) 4667.
[14] E. Rebrov, S. Duinkerke, M. de Croon, J. Schouten, Optimization of heat transfer characteristics, flow distribution, and reaction processing for a microstructured reactor/heat exchanger for optimal performance in platinum catalyzed ammonia oxidation, Chem. Eng. J. 93 (2003) 201.
[15] G. Patermarakis, P. Kerassovitou, Study on the mechanism of oxide hydration and oxide pore closure during hydrothermal treatment of porous anodic Al_2O_3 films, Electrochim. Acta 37 (1992) 125.
[16] R. Spooner, W. Forsyth, X-ray emission spectroscopic study of the sealing of sulfuric acid anodic films on aluminum. I. Technique and application to anodic films, Plating 55 (1968) 336.
[17] K. Wefers, Mechanism of sealing of anodic oxide coatings on aluminum. I. Reasons for reinvestigation, literature, experimental, and results, Aluminum 49 (1973) 553.
[18] S. Desset, O. Spalla, P. Lixon, B. Cabane, Variation of the surface state of α-alumina through hydrothermal treatments, Colloids Surf. A 196 (2002) 1.
[19] F. Shüth, K. Unger, Supported catalysts, in: G. Ertl, H. Knözinger, J. Weitkamp (Eds.), Preparation of Solid Catalysts, Wiley, New York, 1999.
[20] G. Patermarakis, K. Moussoutzanis, J. Chandrinos, Preparation of ultra-active alumina of designed porous structure by successive hydrothermal and thermal treatments of porous anodic Al_2O_3 films, Appl. Catal. A: Gen. 180 (1999) 345.
[21] H. Teunissen, Homogeneous ruthenium catalyzed hydrogenation of esters to alcohols, Chem. Commun. 13 (1998) 1367.
[22] S. Music, S. Popovic, M. Maljkovic, K. Furic, A. Gajovic, Formation of RuO_2 and Ru by thermal decomposition of ruthenium(III)-acetylacetonate, J. Mater. Sci. Lett. 21 (2002) 1131.
[23] Z. Zhong, K. Aika, Effect of ruthenium precursor on hydrogen-treated activated carbon supported ruthenium catalysts for ammonia synthesis, Inorg. Chim. Acta 280 (1998) 183.
[24] J. Mieth, J. Schwarz, Effect of catalyst preparation on the performance of alumina-supported ruthenium catalysts. II. The impact of residual chloride, J. Catal. 118 (1989) 203.
[25] S. Murata, K. Aika, Removal of chlorine ions from Ru/MgO catalysts for ammonia synthesis, Appl. Catal. A: Gen. 82 (1992) 1.
[26] G. Bridger, C. Snowdon, Ammonia synthesis catalysts, in: Catalyst Handbook, Springer-Verlag, New York, 1970.
[27] Z. Kowalczyk, J. Sentek, S. Jodzis, M. Muhler, O. Hinrichsen, Effect of potassium on the kinetics of ammonia synthesis and decomposition over fused iron catalyst at atmospheric pressure, J. Catal. 169 (1997) 407.
[28] Z. Kowalczyk, J. Sentek, S. Jodzis, E. Mizera, J. Goralski, T. Paryjczak, R. Diduszko, An alkali-promoted ruthenium catalyst for the synthesis of ammonia, supported on thermally modified active carbon, Catal. Lett. 45 (1997) 65.
[29] L. Forni, D. Molinari, I. Rossetti, N. Pernicone, Carbon-supported promoted Ru catalyst for ammonia synthesis, Appl. Catal. A: Gen. 185 (1999) 269.
[30] W. Rarog, Z. Kowalczyk, J. Sentek, D. Skladanowski, D. Szmigiel, J. Zielinski, Decomposition of ammonia over potassium promoted ruthenium catalyst supported on carbon, Appl. Catal. A: Gen. 208 (2001) 213.
[31] P. Moggi, G. Albanesi, G. Predieri, G. Spoto, Ruthenium cluster-derived catalysts for ammonia synthesis, Appl. Catal. A: Gen. 123 (1995) 145.
[32] K. Aika, T. Takano, S. Murata, Preparation and characterization of chlorine-free ruthenium catalysts and the promoter effect in ammonia

synthesis 3: a magnesia-supported ruthenium catalyst, J. Catal. 136 (1992) 126.
[33] J. Wellenbüscher, M. Muhler, W. Mahdi, U. Sauerlandt, J. Schütze, G. Ertl, R. Schlögl, Ruthenium supported on zeolite a: preparation and characterization of a stable catalyst for ammonia synthesis, Catal. Lett. 25 (1994) 61.
[34] R. Kojima, K. Aika, Cobalt molybdenum bimetallic nitride catalysts for ammonia synthesis. Part 2. Kinetic study, Appl. Catal. A: Gen. 218 (2001) 121.
[35] C. Jacobsen, S. Dahl, B. Clausen, S. Bahn, A. Logadottir, J. Nørskov, Catalyst design by interpolation in the periodic table: bimetallic ammonia synthesis catalysts, J. Am. Chem. Soc. 123 (2001) 8404.